J. of Fire Prot. Engr., **8** *(1), 1996, pp 31–43*

FACTORS INFLUENCING THE BEHAVIOR OF STEEL COLUMNS EXPOSED TO FIRE

D. Talamona and J. Kruppa
Technical Center of Steel Construction
Domaine St. Paul
Lès Chevreuse, France

J.M. Franssen
Institute of Civil Engineering
University of Liège
Liège, Belgium

N. Recho
Laboratory of Mechanics
and Thermo-Mechanics
of Materials and Structures.
Cedex, France

SUMMARY

Eight tests on eccentrically loaded columns at elevated temperatures were performed at the C.T.I.C.M. Fire Station at Maizière-Les-Metz (France). The results obtained using a finite element code (LENAS) are compared with the results of the fire tests. The eight columns were analyzed with LENAS, which adopts the stress-strain relationship for steel recommended by Eurocode 3, Part 1.2. Calculations were made using data from the tested columns (temperature, yield strength, geometry, applied load, and the initial imperfection) to create a simulation as realistic as possible to compare the calculated critical temperatures with the ones obtained from the fire tests. Some others' calculations were performed using some simplifications. These calculations were made to find out which approximations are acceptable and which are not. A comparison of these different simplifications highlights that the yield strength of the steel section used in the numerical analysis has much more influence on the response of the columns than other characteristics, such as geometrical imperfections, cross-section area, and residual stresses.

INTRODUCTION

The behavior of steel columns submitted to fire has been extensively studied in the last two decades, either by experimental tests or by numerical simulations. A major drawback of the numerical simulations is that they were very often based on elastic perfectly plastic stress-strain relationship and usually ignored the effect of residual stresses. Conclusions presented as general were too often presented from a very limited number of numerical simulations or experimental tests. An important research project was launched in Europe on steel columns submitted to fire which, founded on a very wide numerical and experimental base, should circumvent the aforementioned drawback.

After an extensive research program concerning centrically loaded steel columns[1], the problem of eccentrically loaded columns in fire was considered.

During May 1994, eight tests on eccentrically loaded steel columns subjected to elevated temperatures were performed at

the C.T.I.C.M. Fire Station at Maizières-Lès-Metz. The comparisons between the tests and several analyses made with LENAS[2] (a finite element code) will be presented below. The influence of different parameters such as the yield strength, the geometry, the uniformity of temperature, and the initial imperfection has also been analyzed. The columns were heated with electric flexiheaters, and the temperatures were measured using thermocouples fixed on the columns. More information about the implantation of the thermocouples, the heating programs, and the testing methods is given in the reports[3] of the Fire Station of C.T.I.C.M.

Description of the Tests

The tests that were performed had to satisfy the following conditions:

- The columns tested had to be representative of steel profiles used in construction.
- The temperature had to be uniform in the column. The difference between the highest and the lowest temperatures recorded should not exceed 60° C (and 30° C for the temperatures measured in the same cross-section).
- The temperature, the displacements, and the load had to be recorded with a good precision (and also to have an easy implantation).
- The columns had to be eccentrically loaded.

Experimental Set-Up

The dead weight should not add any lateral imperfection. For this reason the columns were tested vertically. The load was applied eccentrically (see Figure 1). Four transducers of displacement were placed along the columns:

- One for the axial displacement;
- Two for lateral displacement at mid height of the column (in the direction of buckling, as seen in Figures 2a and 2b, displacements D and D');
- One for lateral buckling at mid high of the column. (This measurement allowed to verify that no significant lateral displacement occurred until the moment of failure.)

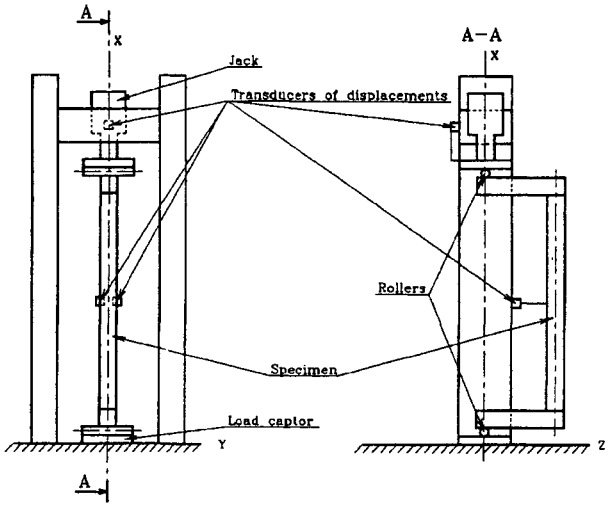

Figure 1. Experimental Set-Up.

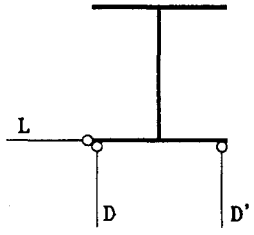

Figure 2a. Buckling Around the Major Axis.

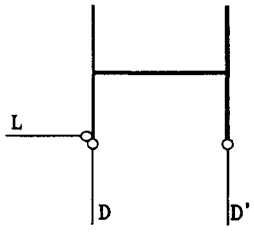

Figure 2b. Buckling Around the Minor Axis.

To facilitate measurement of the displacements and of the temperature, the columns were heated with ceremic mat elements (flexiheaters). The flexiheaters were fixed on the external side of each flange and on one side of the web of the H profiles, using pins welded on the column. The steel profile and the heaters were protected with Rockwool insulation (Figure 3).

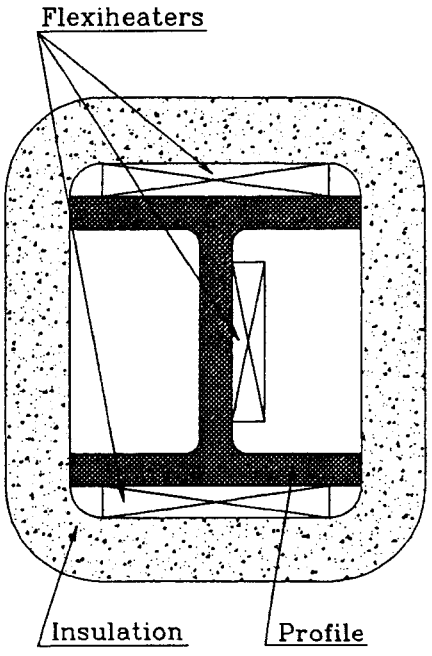

Figure 3. Steel Profile with Flexiheaters and Insulation.

The heat of the resistances was controlled using a P.I.D. (Proportional, Integral, Derivative) controller. Using this kind of heater, controller, and insulation, a better uniformity of the temperature is obtained than in a gas furnace. Using a furnace makes measurement of the displacements very difficult, because of the heating of the wires connected to the column at one end and to the displacement transducers at the other end.

At both ends, the columns were pinned in the direction of bending; rotation was not allowed in the other direction. These end conditions were carried out by two cylinders, so as to prevent lateral buckling of the columns.

Name	P1	P2	P3	P4	P5	P6	P7	P8
Profile	HE200B	HE200B	HE200B	HE200B	HE160M	HE160M	HE140A	HE140A
Test n°	94-S-190	94-S-186	94-S-200	94-S-199	94-S-201	94-S-197	94-S-202	94-S-194
Length (m)	4	4	2	2	2	5	2	5
Slendern.	78.9	78.9	23.4	39.5	27.6	70.6	34.9	87.3
N (kN)	100	100	100	150	100	100	160	100
Ecc. (m)	0.1	0.3	0.65	0.3	0.25	0.5	0.1	0.1
Buck axis.	Weak	Weak	Strong	Weak	Strong	Strong	Strong	Strong
H (mm)	201.4	201.4	201.3	201.4	180.2	180.4	137.49	133.8
B (mm)	200.2	200.3	200.3	200.3	163.4	163.5	141.47	139.8
t_w (mm)	9.04	9.04	9.04	9.04	14	14	5.61	5.61
t_f (mm)	15.04	15	14.96	15	22.68	22.62	8.96	8.28
$\sigma_{mean\_flan.}$	275 MPa	275 MPa	275 MPa	275 MPa	271 MPa	271 MPa	260 MPa	260 MPa
σ_{web}	314 MPa	314 MPa	314 MPa	314 MPa	344 MPa	344 MPa	304 MPa	304 MPa
Δy (mm)	1.5	2.0	1.0	1.0	2.5	1.0	1.0	1.0
Δz (mm)	0.5	3.0	0.5	0.5	3.0	0	0	1.0

Table 1. Applied Loads and Dimensions of the Tested Columns.

Design of the Specimens

The geometry of the columns (profile, length, and axis of buckling) and the loads (load and eccentricity) are described in Table 1.

Before testing the columns, some characteristics were measured, such as :

- The dimensions of the cross section (at the bottom, L/4, L/2, 3L/4, and at the top);
- The initial deformations of the columns on both axes (at L/4, L/2, and 3L/4);
- The yield strength (in the web and in each half of the flanges).

The mean values of the real dimensions of the cross-section, the maximal deformation measured on the columns and the yield strength measured are described in Table 1.

Testing Program

The load was applied at ambient temperature, then maintained constant during the heating. The heating rate was 10° C per minute up to 400° C and only 5° C per minute above 400° C, except for P2 (the first column tested), which had a constant heating rate of 10° C per minute. The uniformity of the temperature on the cross-section and along the column was controlled with several thermocouples (12 thermocouples for the 4-and 5-columns and 6 thermocouples for the 2-columns) of regulation of the heating power. Figure 4 shows the location of the thermocouples on P3. There were 32 thermocouples on this column. Nine thermocouples were welded on section S3 to check for any thermal gradient in the cross-section (and between each faces of the flanges). The temperatures recorded for column P3 (and for the

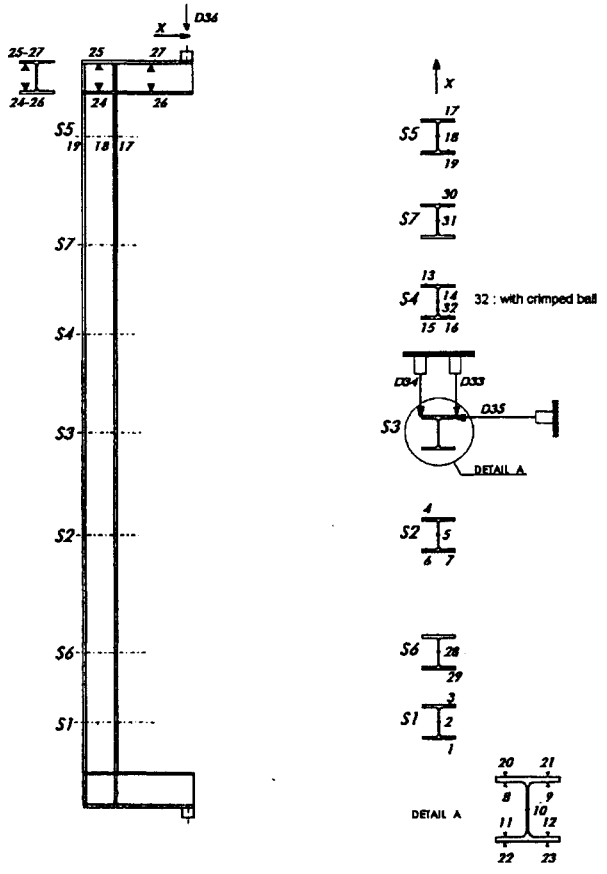

Figure 4. Location of the Thermocouples and the Displacement Sensors on P3.

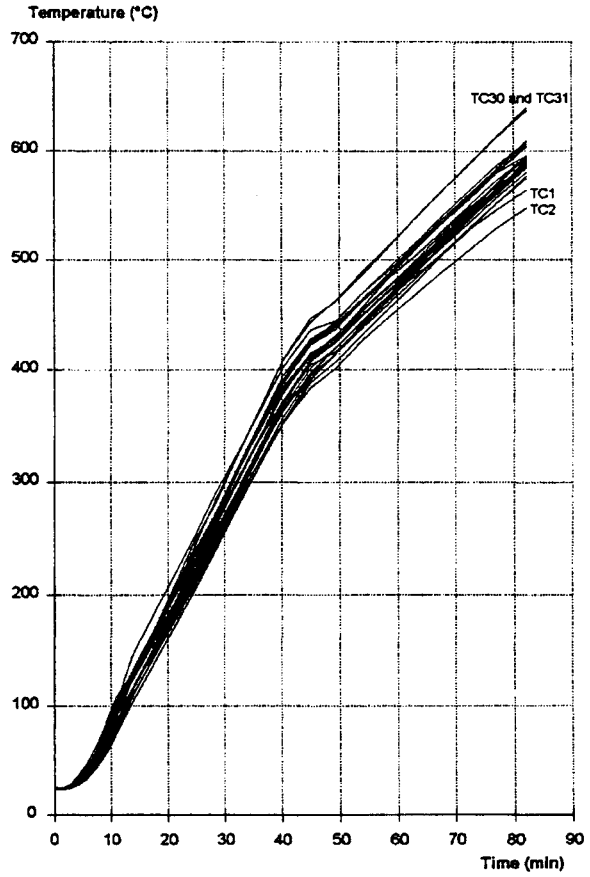

Figure 5. Temperatures Recorded on P3.

thermocouples 1 to 23 and 28 to 32) are plotted on Figure 5. If the temperatures recorded on S1 and S5 are left out, because of loss of heating at the edges of the column (section S1 and S7 are located at 150 mm from the end of the column), the total thermal gradient does not exceed 60° C.

Calculation of the Critical Temperature

The experimental time of collapse has been defined as the moment when the column can no longer support the load. This can be determined by checking the value of the load that was recorded. When the time of collapse is determined, all the temperatures of the thermocouples are known. The critical temperature was calculated using two methods: the mean value of all the thermocouples and the method shown in Equation 1.

$$\theta = \frac{\sum_{i=1}^{n} \theta_i S_i}{\sum_{i=1}^{n} S_i} \qquad (1)$$

S_i represents the area of the web, when the thermocouple is in the web and half the area of one flange when the thermocouple is in a flange.

Lower temperatures were observed in the thermocouples in the sections close to the supports of the column, no doubt the results of heat loss, and so these temperatures were left out of these two calculations.

Test Simulations

LENAS (Large Elasto-plastic Numerical Analysis of Structure) is a finite element code. Calculations can be made by using different material properties such as those defined in the French D.T.U.[4] or the Eurocode 3, Part 1.2.[5].

Description of the Code

LENAS[6,7] is used for the analysis of the behavior of 3D steel structures submitted to fire. In the frame of this project 3D beam elements have been used.

- The Bernoulli hypothesis is considered, *i.e.*, plane sections remain perpendicular to the longitudinal axis and no shear energy is considered.

- The angles between the deformed longitudinal axis and the undeformed but translated longitudinal axis are small, which means:

  $\sin \varphi \cong \varphi$

  $\cos \varphi \cong 1$

  where φ angle between the arc and the cord of a beam element.

The non-linear terms of the strain are considered, except for the Von Karman hypothesis which stands:

$$\frac{1}{2} \frac{\partial u}{\partial x} << 1 \qquad (3)$$

where u = longitudinal displacement,
x = longitudinal coordinate.

- The discretization of the cross-section is made according to the fiber model (quadrilateral fibers). At every longitudinal point of integration, all variables such as temperature, strain, stress, etc., are uniform in each fiber.

- The tangent stiffness matrix is evaluated at each iteration of the convergence process (pure Newton-Raphson method).

- Residual stresses are considered by means of initial—and constant—strains, according to Franssen[8].

- The material behavior in case of strain reversal is elastic, with the elastic modulus equal to the Young's modulus at the origin of the stress-strain curve. The plastic strain is presumed not to be affected by an increase in temperature[9].

In one cross-section, some fibers may therefore exhibit a decreased tangent modulus because they are still on the loading branch, whereas at the same time some other fibers behave elastically.

- The displacement type element is an update Lagrangian description.
- The displacement of the node line is described by the displacements of two nodes (one at each end). Each node supporting three translations, three rotations, and warping.
- The longitudinal integrations are numerically calculated using Lobatto's method and the longitudinal displacements are a linear function of x.

For the simulations presented in this paper, a number of 10 finite elements were used to model the columns, and the time step was chosen as 3.2 minutes.

Material Properties

The calculations were made using Eurocode 3, Part 1.2. material properties described in the subsequent section.

STRESS-STRAIN RELATIONSHIP

The stress-strain relationship of Eurocode 3, Part 1.2. is divided into three zones, shown in Figure 6 and Table 2:

Strain range	Stress σ	Tangent modulus
$\varepsilon < \varepsilon_{p,\theta}$	$\varepsilon \cdot E_{a,\theta}$	$E_{a,\theta}$
$\varepsilon_{p,\theta} < \varepsilon < \varepsilon_{y,\theta}$	$\sigma_{p,\theta} - c + \left(\frac{b}{a}\right) \cdot \left[a^2 - \left(\varepsilon_{y,\theta} - \varepsilon\right)^2\right]^{0,5}$	$\frac{b \cdot \left(\varepsilon_{y,\theta} - \varepsilon\right)}{a \cdot \left[a^2 - \left(\varepsilon - \varepsilon_{y,\theta}\right)^2\right]^{0,5}}$
$\varepsilon_{y,\theta} < \varepsilon < \varepsilon_{u,\theta}$	$\sigma_{y,\theta}$	0
Parameters	$\varepsilon_{p,\theta} = \frac{\sigma_{p,\theta}}{E_{a,\theta}}$	$\varepsilon_{y,\theta} = 0.02$ $\varepsilon_{u,\theta} = 0.2$
Functions	$a^2 - \left(\varepsilon_{y,\theta} - \varepsilon_{p,\theta}\right) \cdot \left(\varepsilon_{y,\theta} - \varepsilon_{p,\theta} + \frac{c}{E_{a,\theta}}\right)$	
	$b^2 - c \cdot \left(\varepsilon_{y,\theta} - \varepsilon_{p,\theta}\right) \cdot E_{a,\theta} + c^2$	
	$c = \frac{\left(\sigma_{y,\theta} - \sigma_{p,\theta}\right)^2}{\left(\varepsilon_{y,\theta} - \varepsilon_{p,\theta}\right) \cdot E_{a,\theta} + 2 \cdot \left(\sigma_{y,\theta} - \sigma_{p,\theta}\right)}$	

Table 2. Stress-Strain Relationship.

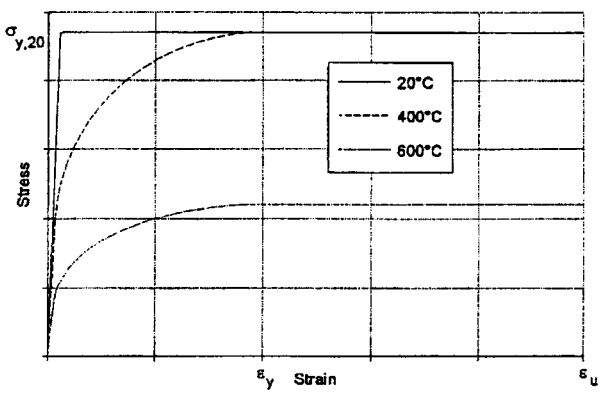

Figure 6. Variation of Stress-Strain Relationship with Temperature according to EC 3, Part 1.2.

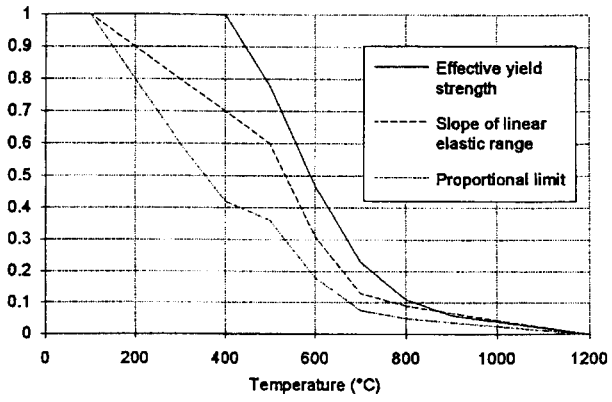

Figure 7. Reduction Factors for Stress-Strain Relationship of Steel at Elevated Temperatures.

- A linear part up to a strain equal to $\sigma_{p,\theta} / E_{a,\theta}$
- An elliptical part up to a strain of 0.02
- A plateau up to a strain of 0.2

EVOLUTION OF THE PROPERTIES WITH THE TEMPERATURE

The evolution of the material properties is given for heating rates between 2 and 50° C/min. For these heating rates, the deformations generated by creep are assumed to be included in the stress-strain relationship. The evolution of the parameters is given in Table 3 and shown in Figure 7.

	$k_{y(\theta)} = \frac{\sigma_{y(\theta)}}{\sigma_{y(\theta)}}$	$k_{p(\theta)} = \frac{\sigma_{p(\theta)}}{\sigma_{p(\theta)}}$	$k_{E(\theta)} = \frac{E_{a(\theta)}}{E_a}$
20°C	1.000	1.000	1.000
100°C	1.000	1.000	1.000
200°C	1.000	0.807	0.900
300°C	1.000	0.613	0.800
400°C	1.000	0.420	0.700
500°C	0.780	0.360	0.600
600°C	0.470	0.180	0.310
700°C	0.230	0.075	0.130
800°C	0.110	0.050	0.090
900°C	0.060	0.0375	0.0675
1000°C	0.040	0.025	0.045
1100°C	0.020	0.0125	0.0225
1200°C	0.000	0.000	0.000

Table 3 : Reductor Factors for the Stress-Strain Relationship of Steel at Elevated Temperatures.

THERMAL ELONGATION $\frac{\Delta L}{L}$

The thermal elongation of steel $\frac{\Delta L}{L}$ may be determined (according to Eurocode 3, Part 1.2), from the following:

$$\frac{\Delta L}{L} = -2.416 \cdot 10^{-4} + 1.2 \cdot 10^{-5} \cdot \theta_a + 0.4 \cdot 10^{-8} \cdot \theta_a^2$$

$20°C \leq \theta < 750°C$ (4)

$$\frac{\Delta L}{L} = 1.1 \cdot 10^{-2}$$

$750°C \leq \theta < 860°C$ (5)

$$\frac{\Delta L}{L} = -6.2 \cdot 10^{-3} + 2 \cdot 10^{-5} \cdot \theta_a$$

$860°C \leq \theta < 1200°C$ (6)

Hypotheses of Calculations

In a first step, calculations were made to simulate the real column as closely as possible (geometry, temperature, yield strength, etc.). In a second phase, the influence of some parameters was checked to find out what kind of simplification would be acceptable and what would not be acceptable.

EXACT ANALYSIS

The first calculations were made to simulate the real column tested as closely as possible. The actual value of the temperature is taken (the temperature is not uniform in the cross-section and along the column and the yield strength is different in the web and in the flanges. In the web, it is equal to the value measured; in the flanges, it is equal to the mean value of the four values measured. (See Table 1.) The following assumptions were made:

- The cross-section of the profile is taken equal to the mean value of the dimensions measured (Table 1).
- The dead weight is not taken into account.
- The residual stresses are taken as a bi-triangular distribution[10] with a maximum value equal to 0.1 x 235 MPa[11].
- The eccentricity is simulated by a finite element perpendicular to the specimen.
- The initial imperfection of the column is taken into account with a sinusoidal deformation. The maximum of this deformation is equal to the value measured (Table 1) and is assumed to be at the center of the column.

The results of these calculations are labeled LENAS-ESS in Figure 8 and Table 4.

APPROXIMATE ANALYSIS

Six other simulations were made for each column. The results of these calculations are given in Table 5 and Figure 9. Table 5 presents the equivalent uniform temperature *i.e.*, the mean value of the temperature of the thermocouples.

For these calculations, the same data as above were used but with some simplifications:

- TEMP : The temperature is uniform in the cross section and along the column.
- GEO : The geometry of the cross section is taken as given in catalogues[12]

COLUMN	P1	P2	P3	P4	P5	P6	P7	P8
θ_{test} (°C)	664	575	599	537	753	572	539	507
$\theta_{LENAS-ESS}$ (°C)	655	540	590	520	716	591	529	507
$\Delta\theta = \theta_{LENAS-ESS} - \theta_{TEST}$ (°C)	-9	-35	-9	-17	-37	+19	-10	+0

Table 4. Comparison LENAS-ESS and TEST.

and the initial imperfection is equal to L/1000.

- SIG1 : σ_y = 235 MPa as given theoretically for a S235 steel profile.
- SIG2 : σ_y is uniform in the cross-section and equal to the $\sigma_{y\_flanges}$ measured for the flanges.
- SIG3 : σ_y is uniform in the cross-section

$$\sigma_y = \frac{\sigma_{y-flanges} S_{flanges} + \sigma_{y-web} S_{web}}{S_{flanges} + S_{web}}$$

with S the area.

- SIMP : The temperature is uniform in the cross-section and along the column, σ_{y_web} is equal to $\sigma_{y\_flanges}$ (see SIG2) and the geometry of the cross-section is taken from catalogue[12] and an initial imperfection of L/1000.

The column called TEST in Table 5 gives the critical temperature of the column during the test performance.

Results

For column P1, the electric power broke down after 86 minutes and came back 4 minutes later. This is the reason Figure 8 (P1) shows no increase of displacement between 86 and 90 minutes. This blackout does not appear in LENAS simulation, because the calculation step was too large, and on the curve there is a linear interpolation between two points. As the transducers were reset, the curve after 90 minutes was "pasted" at the end of the first recording, with an offset equal to the last value recorded.

For column P2, the computer did not record any displacement before 22 minutes. When it started recording, the initial value was zero (the transducer where reset). There was only relative displacement from time t = 22 minutes. An additional displacement equal to the value calculated with LENAS (at t = 22) was added to the data recorded. From zero to 22 minutes, displacement remains constant and equal to the value calculated with LENAS at ambient temperature. For this reason, there is a small step after 22 minutes.

The results of the calculations using LENAS are very close to the measurements during the fire tests. The critical temperatures obtained with LENAS are safer than the tests (See Table 4 and Figure 8), except for column P6 where LENAS gives a temperature 19° C higher than the one measured during this test.

COLUMN	TEST	ESS	GEO	TEMP	SIG1	SIG2	SIG3	SIMP
P1	664	655	654	653	636	655	659	650
P2	575	540	535	536	505	540	545	563
P3	599	590	600	605	530	590	595	611
P4	537	520	519	516	462	520	527	515
P5	753	716	719	726	688	711	722	721
P6	572	591	594	589	565	588	597	590
P7	539	529	508	539	503	525	552	514
P8	507	507	488	514	478	503	511	512

Table 5. Equivalent Critical Temperature of the Columns (°C)

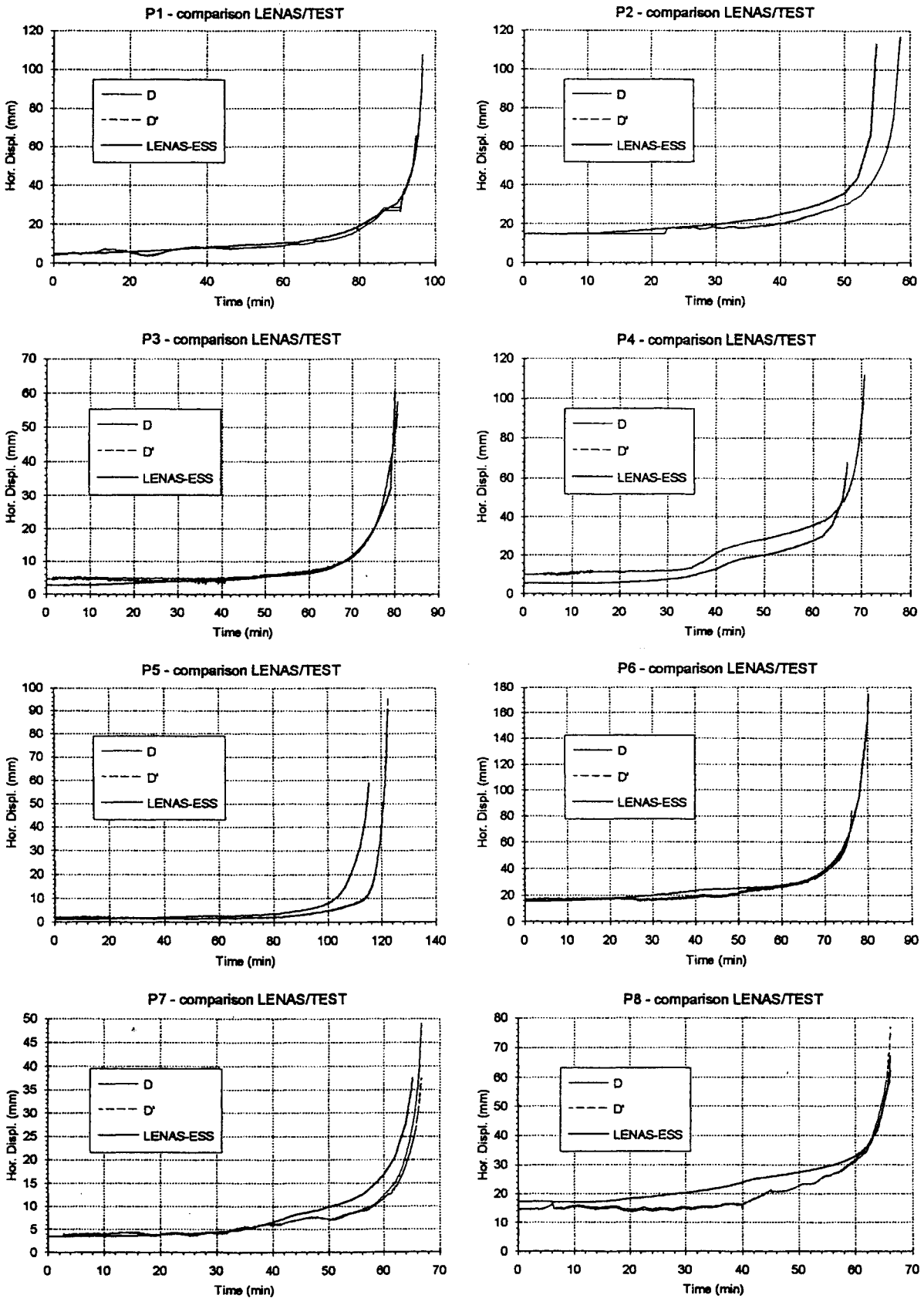

Figure 8. Horizontal Displacements of Columns P1 to P8: Comparison LENAS - TEST.

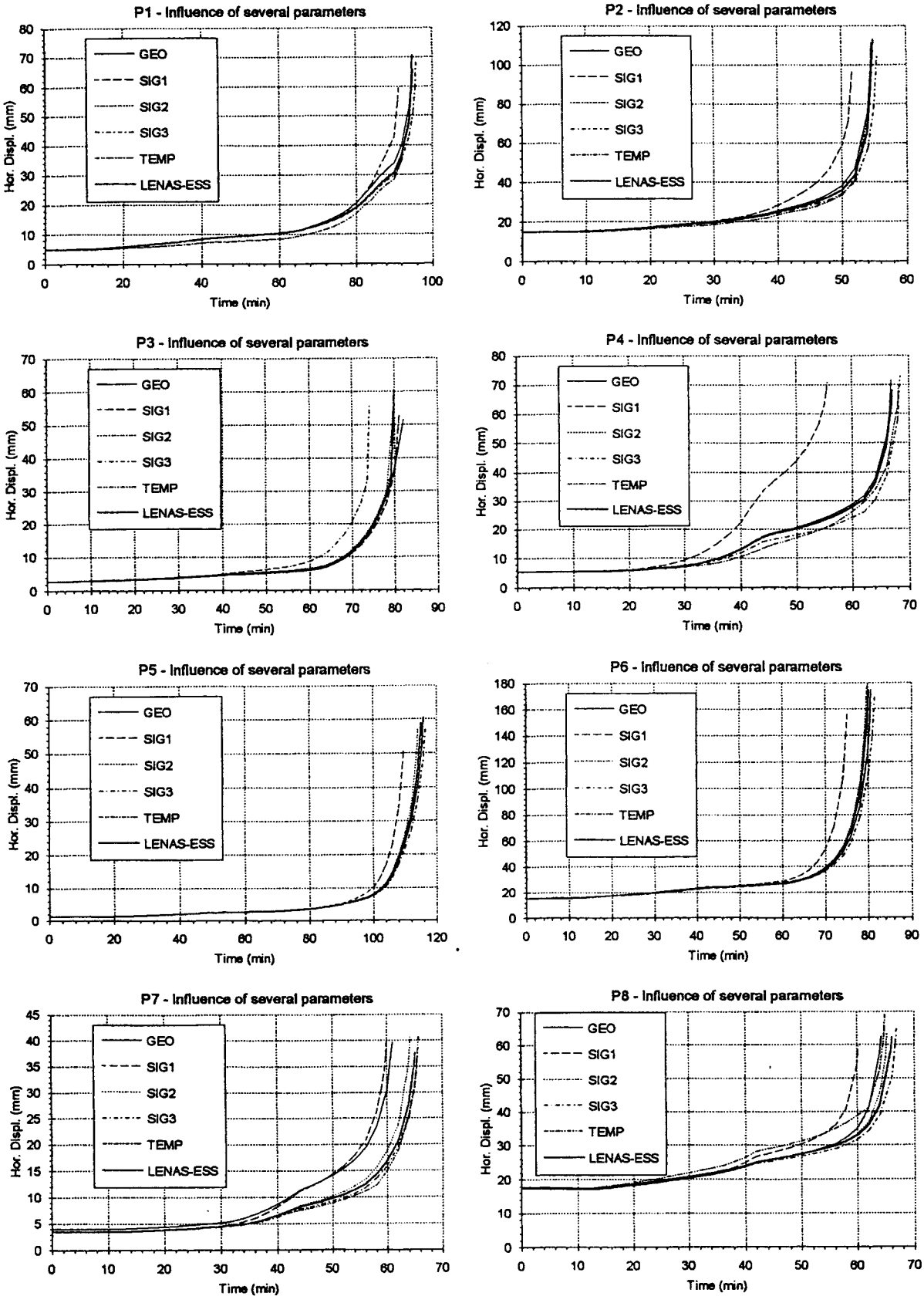

Figure 9. Influence of Several Parameters.

From the six other calculations, it can be concluded that it is acceptable to take:

- The nominal geometry.
- A uniform temperature in the column equal to the mean value of the actual distribution in the central part of the column, *i.e.*, support zones excluded.
- A uniform yield strength in the cross section as defined for SIG2 or SIG3. Note that using s_y equal to the theoretical value of 235 MPa leads to higher discrepancy (on the conservative side, in this test series).

See Figure 9.

Conclusion

LENAS is able to accurately predict the critical temperature of eccentrically loaded columns. Good results were also obtained using some approximations as for SIMP. Among different parameters (such as geometrical imperfections, temperature gradients, sectional area, and yield strength), the last one is clearly the most important and its actual value should be used. The nominal value of the other parameters can be used as a valid approximation.

Ackowledgments

This work was sponsored by the European Convention for Coal and Steel. This research project involves Mr. L. Twilt from TNO in the Netherlands who is investigating the effect of non-symmetric heat exposure and Mr. J.B. Schleich and L.G. Cajot from ProfilARBED in Luxembourg. The authors acknowledge their contribution to the discussions on the subject reported in this paper.

Nomenclature

$\sigma_{y,\theta}$	Effective yield strength at elevated temperature
$\sigma_{p,\theta}$	Proportional limit at elevated temperature
σ_{y_flange}	Effective yield strength in the flanges
σ_{y_web}	Effective yield strength in the web
$E_{a,\theta}$	Slope of the linear elastic range at elevated temperature θ
ε	Strain
$\varepsilon_{p,\theta}$	Strain at the proportional limit
$\varepsilon_{y,\theta}$	Yield strain
$\varepsilon_{u,\theta}$	Ultimate strain
a	Coefficient
b	Coefficient
c	Coefficient
S	Area
θ	Temperature
θ_a	Steel temperature
L	Length
ΔL	Variation of length
N	Axial load
Δ_y	Initial imperfection of the column on y axis
Δ_z	Initial imperfection of the column on z axis
t_f	Flange thickness
t_w	Web thickness
H	Depth of the section
B	Width of the section
u	Longitudinal displacement
x	Longitudinal coordinate
φ	Angle between the arc and the cord of the beam element

REFERENCES

1. Franssen, J.M., Schleich, J.B., and Cajot, L.G., "A Simple Model for the Fire Resistance of Axially Loaded Members According to Eurocode 3," *J. Construct. Steel Research*, Art. No. 1357, 1995.

2. Franssen, J.M., Talamona, D., *et. al.*, "A Comparison Between Five Structural Fire Codes Applied to Steel Elements," *Fourth International Symposium on Fire Safety Science*, Ottawa, June 1994.

3. Test Report No. 94 - S - 186, No. 94 - S - 190, No. 94 - S - 194, No. 94 - S - 197, No. 94 - S - 199, No. 94 - S - 200, No. 94 - S - 201 and No. 94 - S - 202, Station d'Essais du C.T.I.C.M., France, 1994

4. D.T.U. Fire-Steel, "Method of Prediction by Calulation of the Behavior of Steel Structures Subjected to Fire," *Review Construction Métallique*, No. **3**, 1982.

5. pr ENV 1993 - 1 - 2. Eurocode 3 . Design of Steel Structures. Draft Part 1.2. Structural Fire Design, July 1993, Version CEN, 1993.

6. Talamona, D., Buckling of Eccentrically Loaded Columns at Elevated Temperature. Thèse, Université Blaise Pascal, Clermont-Ferrand, pp. 59-87, 1995.

7. Kaneko, H., LENAS-MT, C.T.I.C.M., France, 1989.

8. Franssen, J.M., Modélisation de l'influence des contraintes résiduelles dans les profils métalliques soumis à l'incendie, pp. 35-42, Construction Métallique, No. 3, 1989.

9. Franssen, J.M., "The Unloading of Building Materials Submitted to Fire," pp. 213-227, *Fire Safety Journal*, Elsevier, Vol. **16**, 1990.

10. *Steel Construction - Eurocode 3 :* "Design of Steel Structure" and National Application Document - Part 1.1 : General Rules and Rules for Buildings, 1993.

11. "Buckling Curves of Hot Rolled H Steel Sections Submitted to Fire," Report No. 97.798-2-ME/V, LABEIN, Spain, 1993.

12. ARBED Catalogue, Sales program, Structural Shape, printed 01/1993, Luxembourg.